

# Spatial dependence of time-dependent friction for pair diffusion in a simple fluid

John E. Straub<sup>a)</sup> and Bruce J. Berne

*Department of Chemistry, Columbia University, New York, New York 10027*

Benoît Roux

*Department of Chemistry, Harvard University, Cambridge, Massachusetts 02138*

(Received 1 May 1990; accepted 16 July 1990)

Molecular dynamics simulations are used to determine the time-dependent friction for pair diffusion in an isotropic Lennard-Jones fluid as a function of the separation between two diffusing particles. A numerical method proposed by Straub, Borkovec and Berne is used. It is found that both the initial value and the detailed time-dependence of the friction are dependent on the interparticle separation. The dependence of the pair diffusion coefficient on separation is determined. Comparisons are made with various hydrodynamic and collision theories. The rate constant for diffusion controlled reactions is discussed.

## I. INTRODUCTION

To apply the generalized Langevin equation (GLE)<sup>1,2</sup> to chemical and physical problems one must first determine the dynamic friction coefficient on a molecular bond or on a complicated reaction coordinate. As we have discussed in the preceding paper<sup>3</sup> it does not suffice to know the dynamic friction on all of the atoms because bond friction contains cross correlations ignored by the atomic frictions. Thus to proceed it is necessary to devise realistic models of friction on well-defined collective coordinates in molecules. A detailed discussion of the formalism for calculating dynamic friction coefficients and the approximations used in various treatments is given in the preceding paper in this volume.<sup>3</sup>

Recently, an accurate method for the calculation of time-dependent friction on molecular bonds as a function of the bond length, as well as solvent mass and structure, was presented.<sup>4</sup> This method has already been used to determine the time-dependent friction for a simple isomerization reaction.<sup>5</sup> Detailed knowledge of the time dependence of the friction was found to be important in making accurate theoretical predictions of the rate constant. In the preceding paper<sup>3</sup> we have shown that under circumstances when the motion of the internal coordinate is rapid compared to that of the bath one can compute the friction by assuming that the bond is rigid, but this is not always the case.

Here we present detailed data for the time-dependent friction for a pair of atoms diffusing in an isotropic Lennard-Jones fluid as a function of the separation between the atom pair. This data is used to determine the dependence of the pair diffusion coefficient on separation. The rate constant in the Smoluchowski theory of diffusion controlled reactions is discussed using this data. The data is also used to test the assumption that each atom experiences an independent random force and the amplitude of the mean-square fluctuation is analyzed in terms of the local average solvent density structure around the solute particles. Lastly, we investigate the validity of using the GLE in the Kramers theory of chemical reaction rates and its Grote-Hynes variant.

## II. METHOD

Consider the relative motion of a pair of identical particles in a liquid separated by the distance  $x$ . It is common to assume that the dynamics of this coordinate is correctly described by the generalized Langevin equation (GLE)

$$\mu \ddot{x} = - \frac{\partial W(x)}{\partial x} - \int_0^t dt' \zeta(t') \dot{x}(t-t') + R(t), \quad (2.1)$$

where  $x$  is the coordinate,  $\mu$  is its reduced mass,  $W(x)$  is the potential of mean force for coordinate  $x$ ,  $\zeta(t)$  is the time-dependent friction, and  $R(t)$  is the random force which satisfies the fluctuation-dissipation theorem  $\langle R(t)R(0) \rangle = k_B T \zeta(t)$ . Implicit in Eq. (2.1) is the assumption that the friction experienced by the reaction coordinate is independent of the value of the coordinate  $x$ . Because the pair of atoms executes rotational as well as radial motion, the potential of mean force must include a centrifugal distortion term.<sup>6</sup> It is important to point out that this equation does not spring from any careful derivation from the rigorous classical equations of motion describing the liquid which are perforce highly nonlinear (nonharmonic). In fact, this equation can be derived in general only if it is assumed that the coordinate  $x$  is linearly coupled to a bath of harmonic oscillators in the continuum limit.<sup>7</sup> Nevertheless, this equation has been very useful for delineating a wide variety of liquid state processes. As written, this is a one dimensional GLE. A more complete stochastic theory would contain the coupling between the radial and angular motion of the relative vector. Only when the dynamic friction decays very rapidly compared to the time scale characterizing the reorientation of the pair can one ignore this coupling. This is expected for very dense fluids where the reorientation becomes slow, but it is not valid for low densities or weak coupling with the consequence that the above equation has a limited utility in dealing with the energy diffusion limit. These questions are addressed in the preceding paper in this volume.<sup>3</sup>

A method for the calculation of the time-dependent friction  $\zeta(t)$  as a function of the coordinate  $x$  has recently been presented.<sup>4</sup> In this method, the coordinate is restricted by a harmonic confining potential of frequency  $\omega$  to a region cen-

<sup>a)</sup> Present address: Department of Chemistry, Boston University, Boston, Massachusetts 02215.

tered at  $x = x_0$ . Including potential of mean force effects, the average value of coordinate  $x$  will be  $\langle x \rangle$ . For a harmonic potential of mean force one can derive the following generalized Langevin equation for  $q = x - \langle x \rangle$  as

$$\mu \ddot{q} = -\mu \bar{\omega}^2 q(t) - \int_0^t dt' \zeta(t') \dot{q}(t-t') + R(t) \quad (2.2)$$

where  $\langle q \rangle = 0$ ,  $\bar{\omega}^2 = \beta \mu \langle q^2 \rangle^{-1}$ , and  $\zeta(t)$  is the time-dependent friction on coordinate  $q$ . The corresponding memory function equation is<sup>8</sup>

$$\dot{C}_v(t) = - \int_0^t dt' K(t') C_v(t-t'), \quad (2.3)$$

where the memory function  $K(t)$  is related to the dynamic friction through

$$K(t) = \bar{\omega}^2 + \frac{\zeta(t)}{\mu}, \quad (2.4)$$

where  $C_v(t) = \langle \dot{q}(t) \dot{q}(0) \rangle \langle \dot{q}^2 \rangle^{-1}$  is the velocity autocorrelation function. By calculating  $C_v(t)$  and  $\bar{\omega}^2$  and inverting Eq. (2.3), one can extract the friction on  $q$  for motion near the equilibrium position  $\langle x \rangle$ . The choice of a large confining frequency  $\omega$  limits the motion of the coordinate so that the friction accurately represents the friction at a particular point rather than an average over a region. Of course,  $\omega$  should be chosen small enough to allow for a reasonably large integration time step and such that  $\zeta(t)$  is independent of  $\omega$ .

It has been shown that for pair diffusion of particles in an isotropic Lennard-Jones fluid our method produces good results.<sup>4</sup> The calculated time-dependent friction is independent of  $\omega$ . Furthermore, the time structure, zero-frequency friction, and zero-time value are dependent on the pair separation.

### III. SYSTEM

Our system consists of a box of 64 Lennard-Jones atoms where two atoms represent the diffusing pair solvated by 62 bath atoms. The potential of interaction is

$$U(r) = 4\epsilon \left[ \left( \frac{\sigma}{r} \right)^{12} - \left( \frac{\sigma}{r} \right)^6 \right]. \quad (3.1)$$

Lennard-Jones reduced units are used in which the atomic mass, diameter  $\sigma$ , well depth  $\epsilon$ , and Boltzmann's constant  $k_B$  are equal to unity.  $(m\sigma^2/\epsilon)^{1/2}$  is the unit of time and the reduced number density is  $\hat{\rho} = n\sigma^3$ , where  $n$  is the total number of particles. All our data is for the reduced temperature  $\hat{T} = k_B T/\epsilon = 2.5$  and density  $\hat{\rho} = 1.0$ . This state of our Lennard-Jones system corresponds to a high density fluid.

The time-dependent friction was calculated for nine different interparticle separations as described above. In each case, the time step was 0.02 Lennard-Jones time units and each simulation was run for  $2 \cdot 10^6$  time steps. The velocity autocorrelation function was calculated over the run and the corresponding friction determined using a method similar to that described by Berne and Harp.<sup>1</sup> For each separation, two independent runs were carried out, using different force constants for the confining potential. In each case, the results were independent of the confining potential frequency.

### IV. RESULTS

We have determined the time-dependent friction  $\zeta(t)$  for ten values of the interparticle separation. Table I summarizes the simulation data presenting the time-dependent friction's zero-time value  $\zeta(0)$ , and zero-frequency Laplace transform  $\hat{\zeta} = \hat{\zeta}(0)$  which is related to the diffusion coefficient by the Einstein relation  $D = k_B T/\hat{\zeta}$ . The last column of the table gives the ratio,  $\hat{\zeta}(0)/\zeta(0)$ , of the static friction coefficient  $\hat{\zeta}(0)$  to the initial time value of the dynamic friction constant  $\zeta(t=0)$ . This ratio is the correlation time of  $\zeta(t)$  for the exponential friction model and varies by at most 30% from the average.

Figure 1 shows  $\zeta(t)$  as a function of time as well as the data normalized by the zero-time values; also shown is the time-dependent friction for a single Lennard-Jones atom.<sup>9,10</sup> The inset shows the deviation  $\zeta_{sp}(t)/2 - \zeta(t)$  from the free draining approximation. Clearly, there are large deviations when the bond length is small. As the bond is made longer the deviation goes to zero, as expected. The normalized dynamic friction,  $\zeta(t)/\zeta(t=0)$ , shown in (b) indicates that the initial value of the friction, which is proportional to the mean-square force, is strongly dependent on the interparticle separation. The insets in (b) give the deviation in the calculated normalized frictions,  $[\zeta_{sp}(t)/\zeta_{sp}(t=0) - \zeta(t)/\zeta(t=0)]$ .

The initial decay of  $\zeta(t)$  is well approximated by a Gaussian function,  $\exp(-t^2/2\tau_c^2)$ , where the corresponding correlation time,  $\tau_c$ , does not vary strongly as the interparticle separation is varied. The short time Gaussian decay accounts for between 65% and 75% of the total zero-frequency friction for most separations. (Of course, this assumes that integration of the friction gives an accurate estimation of the long-time collective modes. This being the case,  $\tau_c$  can be determined from equilibrium moments.<sup>21</sup> It is probable that there is an error in this method on the order of 10%.) However, it can be seen that the collective modes of the solvent manifest themselves differently for different separations and the long time decay is dependent on the interparticle separation. The strongest difference between the zero-frequency friction coefficient  $\hat{\zeta}(0)$  at different separations results from the difference in the zero-time values, or the mean-square force. The correlation between  $\hat{\zeta}(0)$  and  $\zeta(0)$  is displayed graphically in Fig. 2. Note that at large separations we expect the friction acting on the interparticle separation to be close to one-half the friction acting on a

TABLE I. Simulation data for the time-dependent friction at various values of the interparticle separation  $a$ , along with the single particle result.

$a$	$\langle x \rangle - a$	$\zeta(0)$	$\hat{\zeta}(0)$	$\hat{\zeta}(0)/\zeta(0)$
0.25	-0.019	466.2	23.4	0.050
0.50	-0.054	290.3	10.1	0.035
0.75	-0.049	274.1	12.6	0.046
1.00	-0.031	303.9	14.0	0.046
1.25	-0.009	367.6	17.5	0.048
1.50	0.012	451.7	21.3	0.047
1.75	0.017	443.6	22.1	0.050
1.90	0.005	407.8	21.9	0.054
2.10	-0.0002	388.3	19.1	0.049
sp	...	823.6	29.1	0.035

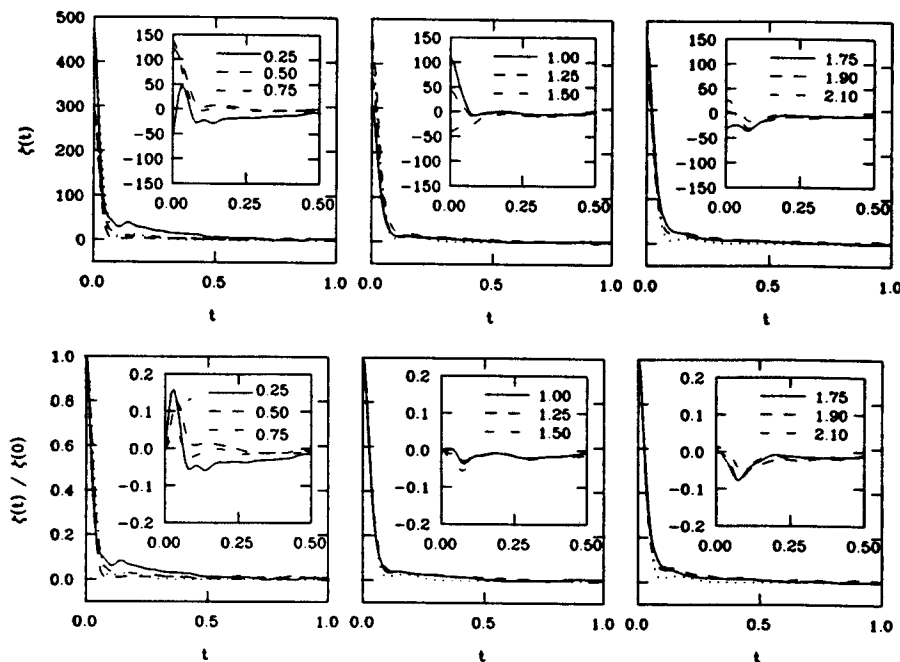


FIG. 1. The time-dependent friction  $\zeta(t)$  as a function of time shown for nine separations (upper). The time-dependent friction  $\zeta(t)$ , normalized by the initial value  $\zeta(0)$ , as a function of time (lower). Shown for comparison is one-half the single-particle friction (dotted line). The insets show the residual difference between the friction and the single particle approximation,  $\zeta(t) - \zeta_{sp}(t)/2$  data normalized by the zero-frequency value.

single particle.<sup>5</sup> The solid line is a least-squares fit to the data which results in the relation  $\hat{\zeta}(0) \approx 0.048 \zeta(0)$ . The square represents the single particle approximation.

The approximately linear relation between  $\hat{\zeta}(0)$  and  $\zeta(0)$ , shown in Fig. 2, indicates that the total friction acting on the reaction coordinate is largely determined by the amplitude of the time-dependent friction  $\zeta(0)$ , i.e., the canonical average of the mean-square force. The overall decay time and shape of the time-dependent friction does not appear to

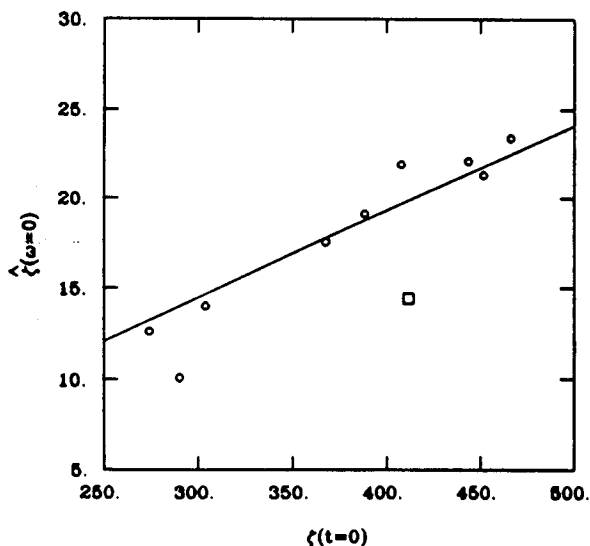


FIG. 2. The correlation of the zero-frequency value of the time-dependent friction  $\hat{\zeta}(0)$  with its initial value  $\zeta(0)$ . The circles represent the correlation for  $\zeta(t)$  while the square corresponds to  $\zeta_{sp}(t)/2$ , the single particle approximation. The solid line is a least-squares fit to the data which results in the relation  $\hat{\zeta}(0) \approx 0.048 \zeta(0)$ .

be strongly sensitive to the pair separation (see Fig. 1). However, even though the initial value of the time-dependent friction does not depend on the dynamics of the LJ pair, preliminary results indicate that the decay time and the absolute value of the total friction are sensitive to the presence of the translational-rotational dynamical coupling of the LJ pair in the fluid.<sup>3</sup>

In Fig. 3 we plot the frequency dependence of the Fourier transform of the time-dependent friction  $\hat{\zeta}(\omega)$  alongside that of the single particle friction. The inset of Fig. 3 shows each data set normalized by its zero-frequency value. Theories of vibrational relaxation in liquids<sup>9</sup> and energy diffusion theories of activated barrier crossing<sup>12,13</sup> rely on an accurate estimate of the frequency dependence of the time-dependent friction. The frequency dependence of the dynamic friction describes how effectively the bath couples to the reaction coordinate oscillating at a particular frequency. Dramatic effects can result from poor coupling between the oscillator and the bath, such as the well known case of very slow vibrational relaxation of  $N_2$  in a rare gas fluid.<sup>9,14,15</sup> Two things are noteworthy about Fig. 3. First, the high frequency tail of the dynamic friction differs from the single particle at small separations ( $r < \sigma$ ) but is in good agreement for larger separations. This point was made recently by Smith and Harris<sup>16</sup> for vibrational relaxation of  $I_2$ . Second, the single particle friction decays more slowly at low frequencies than the true friction.

In Fig. 4 we plot the Laplace transform of the time-dependent friction  $\hat{\zeta}(s)$  as a function of the Laplace variable  $s$  and compare it with that of the single particle friction. The inset of Fig. 4 shows each data set normalized by its zero-frequency Laplace value. While the initial value of the transformed friction depends strongly on the interparticle separation, there is little qualitative difference in the frequency dependence except at low frequencies.

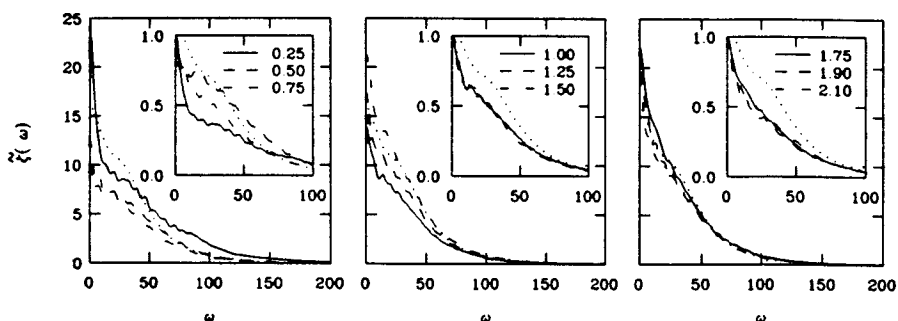


FIG. 3. The frequency dependence of the Fourier transform of the time-dependent friction  $\hat{\zeta}(\omega)$ . The inset shows data normalized by the zero-frequency value.

The theory of Grote and Hynes<sup>17,15</sup> provides the rate constant for the activated crossing of an inverted harmonic potential barrier with frequency  $\omega_B$  in the presence of a time-dependent friction  $\zeta(t)$ . The rate constant is

$$k_{\text{GH}} = \frac{\lambda_r}{\omega_B} k_{\text{TST}} \quad (4.1)$$

where  $\lambda = \lambda_r$  is the reaction frequency which is the positive root of the equation

$$\omega_B^2 - \lambda^2 = \lambda \hat{\zeta}(\lambda) \quad (4.2)$$

and  $k_{\text{TST}}$  is the transition state theory rate constant. In the adiabatic limit, the reaction frequency is low compared to the decay frequency of the friction,  $\hat{\zeta}(\lambda_r) \approx \hat{\zeta}(0)$  and Eq. (4.1) reduces to the Kramers rate.<sup>18</sup> When the barrier frequency is high compared to the decay frequency of the friction Eq. (4.1) reduces to the one-dimensional transition state theory rate constant. At intermediate barrier frequencies, the detailed dependence of  $\hat{\zeta}(s)$  is important in determining the rate constant for barrier crossing in the intermediate and high friction regimes. The inset of Fig. 4 indicates that the  $s$ -dependence of the Laplace transform of the friction normalized by the zero frequency value is relatively independent of the interparticle separation. However, the zero-frequency value is sensitive to the separation. It is therefore important to determine the friction in the barrier region,<sup>5,4</sup> as opposed to approximating the friction by its value in the reactant or product state. We return to this later.

Figure 5 shows a plot of  $\omega_B^2 - \lambda^2$  and  $\lambda \hat{\zeta}(\lambda)$  versus  $\lambda$  for different values of the barrier frequency,  $\omega_B$ . The intersection of the two curves gives the solution of Eq. (4.2). At low frequencies, one observes a large variation of the predicted barrier crossing transmission rate with the bond length, a

result mainly due to bond length dependence of the static friction. At higher barrier frequencies, there is not much of a variation with bond length. Because the free draining approximation to the friction coefficient deviates from the true friction coefficient for realistic bond lengths, the rate constant predicted using this free draining limit will be poor at lower barrier frequencies and will improve with increasing barrier frequency.

The zero-time value for the time-dependent friction is proportional to the mean-square force and can be expressed as

$$\zeta(0) = \beta [ \langle \mathbf{F}_{\text{AB}}(\mathbf{r}_{\text{AB}}) \mathbf{F}_{\text{AB}}(\mathbf{r}_{\text{AB}}) \rangle - \langle \mathbf{F}_{\text{AB}}(\mathbf{r}_{\text{AB}}) \rangle \langle \mathbf{F}_{\text{AB}}(\mathbf{r}_{\text{AB}}) \rangle ], \quad (4.3)$$

where  $\beta = 1/k_B T$ ,  $\mathbf{F}_{\text{AB}}(\mathbf{r}_{\text{AB}})$  is the fluid force acting along the interparticle separation  $\mathbf{r}_{\text{AB}}$  and  $\langle \dots \rangle$  indicates an equilibrium average over the canonical ensemble. The linear correlation between the total static friction and the zero-time value of the time-dependent friction  $\zeta(0)$ , observed in Fig. (2), implies that one can understand variations in the diffusion coefficient in terms of an equilibrium average of the mean-square force. In Fig. 6 we display the zero-time value of the time-dependent friction  $\zeta(0)$  as a function of the interparticle separation. The amplitude of the zero-time value varies by a factor of two over distances corresponding to a few particle radii. Asymptotically, we expect that the mean-square force acting on the interparticle separation should approach one-half the mean-square force acting on a single particle. We expect a value for  $\zeta(t=0)$  of roughly 412 for  $r = \infty$  based on the single particle friction. From the curve we see that this is already achieved for  $\langle x \rangle > 2.1$  to a good approximation.

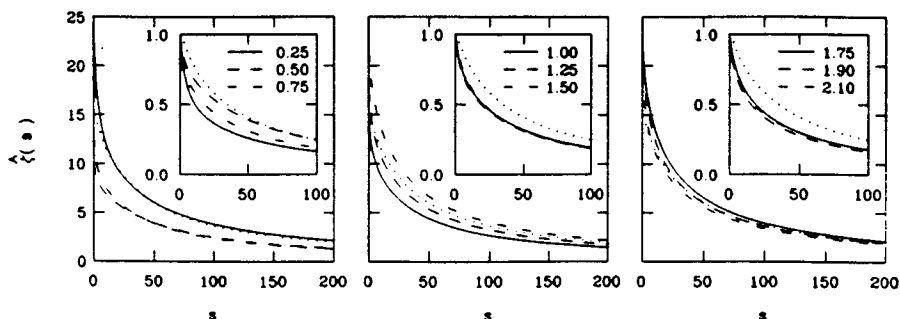


FIG. 4. The frequency dependence of the Laplace transform of the time-dependent friction  $\hat{\zeta}(s)$ . The inset shows data normalized by the zero-frequency value.

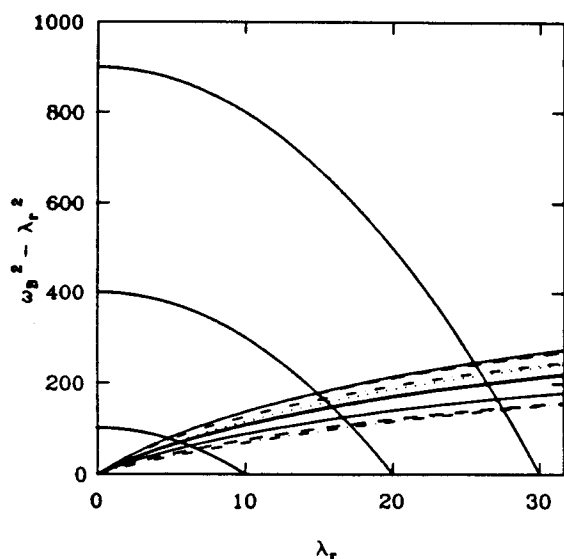


FIG. 5. A graphical solution of the Grote-Hynes equation (4.2). We display curves for all nine pair separations along with the single particle approximation. Three different barrier frequencies are shown,  $\omega_B = 10, 20,$  and  $30$ .

To further understand the origin of the variations in the mean square force, we rewrite the mean-square force fluctuation in Eq. (4.3) in terms of the average solvent density around the solute particles.

$$\beta [\langle \mathbf{F}_{AB} \mathbf{F}_{AB} \rangle - \langle \mathbf{F}_{AB} \rangle \langle \mathbf{F}_{AB} \rangle] = -\Delta W''(\|\mathbf{r}_{AB}\|) - \frac{1}{2} \left\langle \frac{\partial}{\partial \mathbf{r}'_A} \frac{\partial}{\partial \mathbf{r}_A} V_{SA} \right\rangle,$$

where  $\Delta W(\|\mathbf{r}_{AB}\|) = W(\|\mathbf{r}_{AB}\|) - V_{AB}(\|\mathbf{r}_{AB}\|)$  is the cavity potential [see Eqs. (A9) and (A12) and calculational details described in the Appendix]. The integrand of this equation provides insight into the microscopic origin of the

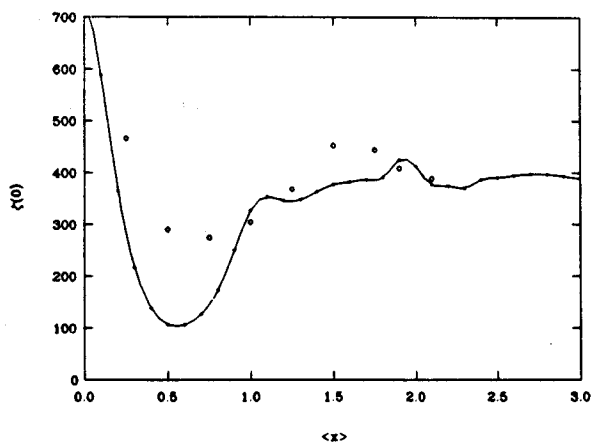


FIG. 6. The zero-time value of the time-dependent friction  $\zeta(0)$  as a function of the interparticle separation. The results from computer simulation (O) are compared with those of the analytic mean-square force of Eq. (A.12) (—). We expect a value of  $\zeta(0) \approx 412$  for  $r = \infty$  based on the single particle friction.

fluctuating collisional forces acting on the reaction coordinate in terms of the local equilibrium solvent density found around the fixed solute particles.

The key approximation to estimate the integral in Eq. (A9) is the superposition approximation for the three point distribution function.<sup>19</sup> It is necessary because the convergence of the averaged multidimensional distribution function  $\rho(x,y)$  is not sufficient to be useful using the present simulation data. The results are plotted in Fig. 6 as a function of the interparticle separation  $\langle x \rangle$  and compared with the results of our simulation. There is reasonable agreement in both the magnitude of the interaction and the qualitative behavior as a function of the interparticle separation. The disagreement between the simulation results and the prediction of Eq. (4.3) is probably due to the breakdown of the superposition approximation as the solute particles begin to overlap. The total interaction potential of the solute with the fluid is then  $2V_{SA}$ . However, the mean-force potential around the overlapped solutes is certainly not  $-2W(r)$ , which is the result of the superposition approximation  $g(r)g(r) = \exp[-2W(r)]$ . In the region where the particles cannot overlap,  $r > \sigma$ , the agreement is much better.

The contour plots show that the amplitude of the collisional impact, an important factor in determining the total friction acting on the reaction coordinate, is largely controlled by the local solvent structure in the vicinity of the solute particles. For example, the increase in the pair diffusion constant observed at a separation of  $0.5\sigma$  is seen to be due to a shielding of the solute particles from the solvent collisional forces. The variation in the mean-square force on the solute pair separation shows that the local solvent structure plays a crucial role in determining the character of the fluctuating forces acting on solutes separated by microscopic distances. This observation casts doubt upon the representation of solvent frictional effects in terms of a continuum model, such as in the hydrodynamic description of the frictional forces often used in Brownian dynamics simulations.<sup>20</sup>

In Fig. 7 we show the static friction coefficient,  $\hat{\zeta}(0)$ , as a function of the interparticle separation. In Fig. 8 we show the relative or pair diffusion coefficient  $D = k_B T / \hat{\zeta}(0)$  as a function of the interparticle separation. We find that the zero frequency value of the friction is correlated with the zero-time value (see Fig. 2) indicating that the contribution of the short time collisional part of the friction dominates the diffusion constant at this temperature and pressure.

In closing this section it is worth noting that it is a relatively simple matter to go beyond predicting the zero-time value of the friction. As shown by Berne and Harp,<sup>1,21</sup> if an ansatz is made for the functional form of the memory function, the parameters in that functional form can then be determined from the equilibrium moments. Berne and Harp<sup>1,21</sup> discussed single particle memory functions for translational and rotational motions and assumed Gaussian memory functions. Here instead one can use Eq. (2.4) together with a Gaussian functional form for  $\zeta(t)$ . Equilibrium moments will then give the two parameters necessary to determine the Gaussian completely. These two parameters will of course be dependent on the bond length. Brooks and

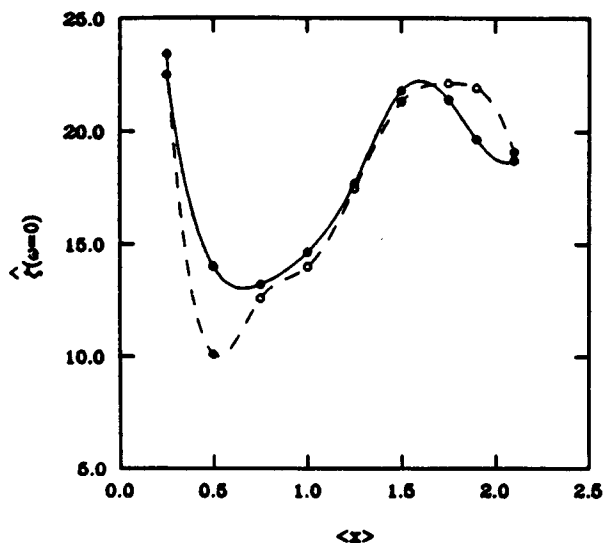


FIG. 7. The zero-frequency value of the Laplace transform of the time-dependent friction  $\hat{\zeta}(\omega=0)$  as a function of the interparticle separation ( $\circ$ ) along with a spline fit to the data (—). The approximate relation  $\hat{\zeta}(\omega=0) = 0.048 \zeta(0)$  from Fig. 6 is shown for comparison. We expect a value of  $\hat{\zeta}(\omega=0) \approx 14.5$  for  $r = \infty$  based on the single particle friction.

Adelman<sup>22</sup> have used this approach to model liquid state reactions.

## V. DISCUSSION

There are many studies of pair diffusion which have increased our understanding of the role of cross-correlation in the velocity correlation function and its contribution to the pair diffusion coefficient in atomic fluids. All of these studies tag atom pairs in the fluid which have a certain interparticle separation distance and then calculate the mean-square displacement and velocity correlation function for the interparticle separation as a function of time and initial separation. From this data, one constructs time-dependent pair-distribution functions and follows their time evolution in terms of simple diffusion schemes<sup>23</sup> or cross-correlations of the velocity correlation function. The cross-correlations can be interpreted in terms of momentum transfer to the solvent cage surrounding the diffusing pair.<sup>24</sup> For several Lennard-Jones state points (all lower in temperature and density than ours) it is found that  $D < 2D_{sp}$  and that the difference between the pair and single particle diffusion is small.<sup>25</sup> The reduction in the pair diffusion coefficient is shown to be a direct result of velocity cross-correlation absent in the single particle approximation.

Our study is the first to directly calculate the pair diffusion coefficient as a function of the pair interparticle separation. We find that for separations  $r > \sigma$  the pair diffusion coefficient  $D(r) < 2D_{sp}$  in agreement with previous results.<sup>25</sup> However, there is a variation of a factor of two in  $D(r)$  over the full range of  $r$ , and for  $0.5\sigma < r < \sigma$ ,  $D(r) > 2D_{sp}$ .

We find that the strong variation in  $D(r)$  is well correlated with the mean-square force on the interparticle separa-

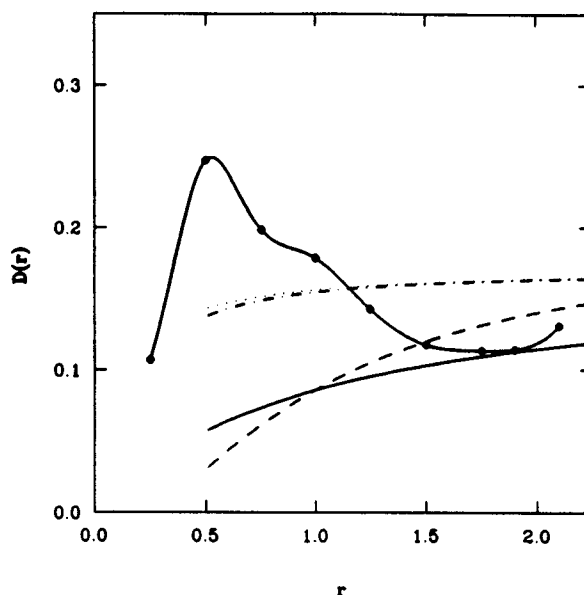


FIG. 8. The diffusion coefficient as a function of the interparticle separation calculated from the Einstein relation  $D = k_B T / \zeta$ . Shown for comparison are other empirical functions proposed to model the spatial dependence of the diffusion coefficient. (—) Eq. (5.1), (--) Eq. (5.3), (-.-) Eq. (5.2) and (···) Eq. (A.13).

tion. At small separations, there is substantial shielding of this force by the other member of the pair. Relating these shielding effects to the solvent accessible solute surface area may provide qualitative rules for the analysis of more complex solutes. This leads to a difference in the zero-frequency friction and in the pair diffusion coefficient. In their study of  $I_2$  vibrational relaxation in Xe, Smith and Harris find that the force correlation on the vibrational coordinate is similar to that for the center-of-mass motion and that cross-correlations lead to differences only at low frequencies. Our results are similar. Figures 3 and 4 show that the high frequency decay is similar for the pair and the single particle approximation, and that the principle difference is in the zero-frequency value and decay at low frequencies.

### A. Models for $D(r)$

Models have been proposed previously to account for the spatial dependence of friction constants for pair diffusion. One of the most common forms uses the Oseen tensor. In the free draining limit, the diffusion constant can be written

$$D(r) = \frac{k_B T}{\zeta(r)} = \frac{k_B T}{\zeta} \left[ 1 + \frac{\zeta}{6\pi\eta r} \right]^{-1}, \quad (5.1)$$

where  $\zeta = \hat{\zeta}(0)$  and  $\eta$  is the solvent viscosity. We use the Enskog value,  $\eta = 1.54$  for a Lennard-Jones fluid at this density  $\hat{\rho} = 1.0$ .<sup>19</sup>

The Oseen tensor is derived from hydrodynamic equations which are valid only for separations very large compared to the particle diameter  $\sigma$ ; that is,  $r \gg \sigma$ . However, we consider it since it is often applied to close interactions, and its form is similar to that of other models summarized below.

Another form, which is quite similar to the Oseen ten-

sor, has been proposed. It is based on empirical fits to computer simulation data for relative diffusion of atoms in a two-dimensional simple fluid<sup>26</sup>

$$D(r) = \frac{2k_B T}{\zeta_{sp}} \left[ 1 - 0.1 \frac{\sigma}{r} \right] \quad r < 3\sigma$$

$$= \frac{2k_B T}{\zeta_{sp}} \left[ 0.8 + 0.5 \frac{\sigma}{r} \right] \quad r > 3\sigma, \quad (5.2)$$

where  $\zeta_{sp} = \hat{\zeta}_{sp}(0)$  is the zero-frequency friction of a single Lennard-Jones atom.<sup>27</sup> Northrup and Hynes have suggested a similar form in their study of rate constants for diffusion controlled ion pair recombination<sup>28,29</sup>

$$D(r) = \frac{k_B T}{\zeta} \left[ 1 - \frac{1}{2} e^{-(r-\sigma)/\sigma} \right]. \quad (5.3)$$

We find the spatial dependence of the zero-frequency friction to vary the diffusion constant within a factor of two over the range  $0 < r < 2.25\sigma$ . Our data indicates that the diffusion constant should *increase with decreasing distance* over the range from  $0.5\sigma < r < 1.7\sigma$  mostly as a result of variations in  $\zeta(0)$  due to solvent shielding effects. All of the models presented above predict that the diffusion constant should *decrease with decreasing distance* over this range. Kapral and coworkers have evaluated a kinetic theory expression for a pair friction tensor.<sup>30</sup> Their calculation for a density  $\hat{\rho} = 0.555$  predicts a friction coefficient acting along the interparticle separation which is similar to the zero-frequency friction displayed in Fig. 7.<sup>31</sup> In particular, they find the friction constant is *increasing* for  $\sigma < r < 2\sigma$  and shows a maximum at  $r = 2\sigma$ . Our data, taken at the higher density  $\hat{\rho} = 1.0$ , shows a maximum close to  $r = 1.7\sigma$ .

It is important to note that the simulations reported here are for small periodic systems. The hydrodynamic interaction reflects this periodic boundary condition in our system. Equation (5.1) on the other hand springs from the far field asymptotic form of the hydrodynamic interaction. Thus, our simulation will never give the limiting form of Eq. (5.1). Strictly speaking, one should compare our results with periodic hydrodynamics in the spirit of Wood and Erpenbeck.<sup>32</sup> Of course, for diffusion controlled reactions the dominant contribution comes from short range effects and thus hydrodynamic limits are not expected to be important.

## B. Rate constants for pair diffusion

Using the various forms for  $D(r)$ , studies of diffusion limited reactions have been made.<sup>28,33,31</sup> The rate constant takes the form

$$k^{-1} = \int_{\sigma}^{\infty} dr \frac{1}{4\pi r^2 g(r) D(r)}, \quad (5.4)$$

where  $g(r)$  is the atomic pair-correlation function.

We have calculated the diffusion limited rate constant in several approximations. (1) Using Eq. (5.4) with our numerically determined diffusion constant (see Fig. 8) for  $\sigma < r < 2.25\sigma$  and  $D(r > 2.25\sigma) = D(r = 2.25\sigma)$ ;  $k = 0.65$ . (2) Approximating the pair diffusion constant as twice the value of the single particle diffusion constant  $D = D_{sp} = k_B T / \zeta_{sp}$ ;  $k = 0.49$ . (3) Using Eq. (5.3) for  $D(r)$ ;  $k = 0.64$ . (4) Using the Smoluchowski result for a flat

potential and  $D = 2D_{sp}$ ;  $k = 4\pi D\sigma = 2.16$ . The integrand of Eq. (5.4) is shown for the calculated positional dependent diffusion coefficient  $D(r)$  and the single particle approximation  $D_{sp}$  in Fig. 9. Here it is clear that the difference in the integrand is greatest in the region  $1.25\sigma < r < 2\sigma$ .

Northrup and Hynes found that short range caging effects induced by the distance dependence of the diffusion constant are small.<sup>28</sup> The strongest spatial dependence in the integrand is due to potential of mean force effects in the radial distribution function. Our calculations support their conclusions.

## VI. CONCLUSIONS

We find that for a pair of atoms in a simple fluid, (1) the zero-time value of the friction is strongly dependent on the interparticle separation, (2) the short time decay of the friction is Gaussian with a collisional decay time which is largely independent of the interparticle separation, (3) the long time hydrodynamic tail, due to collective modes of the solvent, is dependent on the interparticle separation and not well modeled by any empirical or hydrodynamic theories previously proposed, (4) the frequency dependence of the zero-time normalized friction is not strongly dependent on interparticle separation, and (5) that in the range  $0.5\sigma < r < 1.7\sigma$  the diffusion constant should increase with decreasing distance showing a maximum near  $r = 1.7\sigma$ , due to a shielding of the solvent force by the other member of the pair, in qualitative agreement with earlier kinetic theory calculations at lower density.<sup>30</sup>

## APPENDIX

In this appendix, we calculate the mean-square fluctuation in the force acting along the interparticle separation of a diatomic molecule in a simple fluid. The diatomic is made

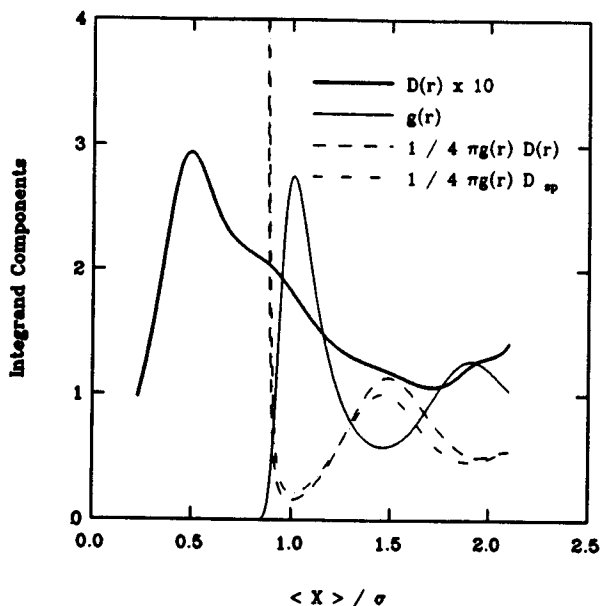


FIG. 9. Components of the integrand for Eq. (5.4) are shown as a function of distance.

of atoms A and B at a fixed separation. Atom A is at the origin and atom B is at position  $(a,0,0)$  in cylindrical coordinates  $(z,\theta,\phi)$ . We assume that the diatomic is homonuclear.

The potential of interaction for the diatomic and fluid can be written

$$V_{TOT} = V_{SS}(\mathbf{r}_S) + V_{SA}(\mathbf{r}_S, \mathbf{r}_A) + V_{SB}(\mathbf{r}_S, \mathbf{r}_B) + V_{AB}(\mathbf{r}_A, \mathbf{r}_B), \quad (A1)$$

where the S stands for all solvent atoms, and A and B for atoms A and B in the diatomic. The total force acting on atom A is

$$\mathbf{F}_A = -\frac{\partial V_{TOT}}{\partial \mathbf{r}_A} = -\frac{\partial V_{SA}}{\partial \mathbf{r}_A} - \frac{\partial V_{AB}}{\partial \mathbf{r}_A} \quad (A2)$$

and similarly for  $\mathbf{F}_B$ .

We can write the average force acting on the interparticle separation between particles A and B as

$$\langle \mathbf{F}_{AB}(\mathbf{r}_{AB}) \rangle = \frac{1}{2} \langle \mathbf{F}_B - \mathbf{F}_A \rangle. \quad (A3)$$

Transforming to center-of-mass and relative coordinates and differentiating with respect to  $\mathbf{r}_{AB} = \mathbf{r}_A - \mathbf{r}_B$ , ( $2\partial/\partial \mathbf{r}_{AB} = \partial/\partial \mathbf{r}_A - \partial/\partial \mathbf{r}_B$ ) we find

$$\begin{aligned} \frac{\partial}{\partial \mathbf{r}_{AB}} \langle \mathbf{F}_{AB}(\mathbf{r}_{AB}) \rangle &= \left\langle \frac{\partial}{\partial \mathbf{r}_{AB}} \mathbf{F}_{AB}(\mathbf{r}_{AB}) \right\rangle \\ &+ \beta [ \langle \mathbf{F}_{AB}(\mathbf{r}_{AB}) \mathbf{F}_{AB}(\mathbf{r}_{AB}) \rangle \\ &- \langle \mathbf{F}_{AB}(\mathbf{r}_{AB}) \rangle \langle \mathbf{F}_{AB}(\mathbf{r}_{AB}) \rangle ], \end{aligned} \quad (A4)$$

where  $\beta = 1/k_B T$ . We want to calculate the fluctuation in the force, the component in the square brackets, by calculating the first two terms.

The first term in Eq. (A4), the derivative of the average force, can be written in terms of the potential of mean force  $W(\mathbf{r}_{AB})$

$$\frac{\partial}{\partial \mathbf{r}_{AB}} \langle \mathbf{F}_{AB}(\mathbf{r}_{AB}) \rangle = -\frac{\partial}{\partial \mathbf{r}_{AB}} \frac{\partial}{\partial \mathbf{r}_{AB}} W(\mathbf{r}_{AB}). \quad (A5)$$

In our cylindrical coordinate system,  $\mathbf{r}_{AB}$  is directed along the z-axis. Writing the full tensor of the second derivative of  $W(\mathbf{r}_{AB})$

$$\begin{aligned} \frac{\partial}{\partial x_i} \frac{\partial}{\partial x_j} W(\mathbf{r}_{AB}) &= -W''(\mathbf{r}_{AB}) \frac{x_i}{\|\mathbf{r}_{AB}\|} \frac{x_j}{\|\mathbf{r}_{AB}\|} \\ &+ \frac{W'(\mathbf{r}_{AB})}{\|\mathbf{r}_{AB}\|} \left( \delta_{ij} - \frac{x_i}{\|\mathbf{r}_{AB}\|} \frac{x_j}{\|\mathbf{r}_{AB}\|} \right), \end{aligned} \quad (A6)$$

the second derivative projected along the interparticle separation (z-axis) is

$$-\hat{z} \cdot \frac{\partial}{\partial \mathbf{r}_{AB}} \frac{\partial}{\partial \mathbf{r}_{AB}} W(\mathbf{r}_{AB}) \cdot \hat{z} = -W''(\mathbf{r}_{AB}). \quad (A7)$$

The second term in Eq. (A4), the average derivative of the force, can be written

$$\begin{aligned} \left\langle \frac{\partial}{\partial \mathbf{r}_{AB}} \mathbf{F}_{AB}(\mathbf{r}_{AB}) \right\rangle &= \frac{1}{2} \left\langle \frac{\partial}{\partial \mathbf{r}_{AB}} (\mathbf{F}_B - \mathbf{F}_A) \right\rangle \\ &= -\frac{1}{4} \left\langle \frac{\partial}{\partial \mathbf{r}_A} \frac{\partial}{\partial \mathbf{r}_A} V_{SA} \right\rangle \end{aligned}$$

$$\begin{aligned} &- \frac{1}{4} \left\langle \frac{\partial}{\partial \mathbf{r}_B} \frac{\partial}{\partial \mathbf{r}_B} V_{SB} \right\rangle \\ &+ \left\langle \frac{\partial}{\partial \mathbf{r}_B} \frac{\partial}{\partial \mathbf{r}_B} V_{AB}(\|\mathbf{r}_{AB}\|) \right\rangle. \end{aligned} \quad (A8)$$

There are no cross terms, since  $V_{SA}$  is independent of  $\mathbf{r}_B$  and  $V_{SB}$  is independent of  $\mathbf{r}_A$ . The third term on the right is the average of the second derivative of the direct potential between the atoms of the diatomic. The first and second terms are equivalent.

Combining Eqs. (A5) and (A8) with Eq. (A4) provides us with the final expression for the fluctuation in force projected along the interparticle separation (z-axis)

$$\begin{aligned} \beta \hat{z} \cdot [ \langle \mathbf{F}_{AB} \mathbf{F}_{AB} \rangle - \langle \mathbf{F}_{AB} \rangle \langle \mathbf{F}_{AB} \rangle ] \cdot \hat{z} \\ = -\Delta W''(\|\mathbf{r}_{AB}\|) - \frac{1}{2} \left\langle \frac{\partial}{\partial z_A} \frac{\partial}{\partial z_A} V_{SA} \right\rangle, \end{aligned} \quad (A9)$$

where  $\Delta W(\|\mathbf{r}_{AB}\|) = W(\|\mathbf{r}_{AB}\|) - V_{AB}(\|\mathbf{r}_{AB}\|)$  is the cavity potential.

The calculation of the average second derivative of  $V_{SA}(\|\mathbf{r}_A\|)$  involves an integral over all space occupied by solvent with respect to particle A. The component acting along the interparticle separation is

$$\begin{aligned} \frac{\partial}{\partial z_A} \frac{\partial}{\partial z_A} V_{SA} |_{r_A=z} \\ = V_{SA}'' \cos^2 \theta + \frac{V_{SA}'}{r} (1 - \cos^2 \theta) = \sum(r, \theta), \end{aligned} \quad (A10)$$

where  $r$  is the radial distance from particle A to a position in the solvent (see Fig. 10). The integral over space can then be written

$$\begin{aligned} \left\langle \frac{\partial}{\partial z_A} \frac{\partial}{\partial z_A} V_{SA} \right\rangle \\ = \rho \int d^3r g^{(3)}(\mathbf{r}) \left[ V_{SA}'' \cos^2 \theta + \frac{V_{SA}'}{r} (1 - \cos^2 \theta) \right] \\ = \rho \int d^3r g^{(3)}(\mathbf{r}) \sum(r, \theta) \end{aligned}$$

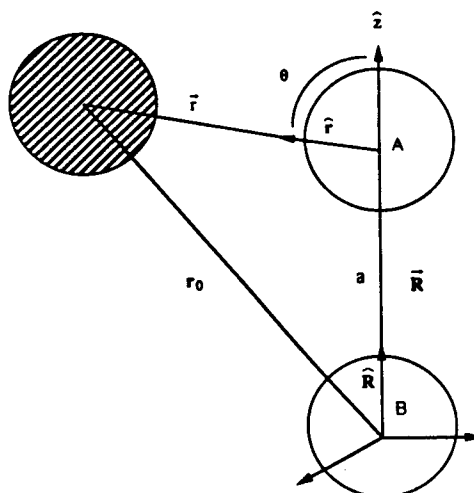


FIG. 10. Coordinate system and particle placement for calculation of mean-square force on a single particle with a second particle fixed a distance  $r = a$  away.



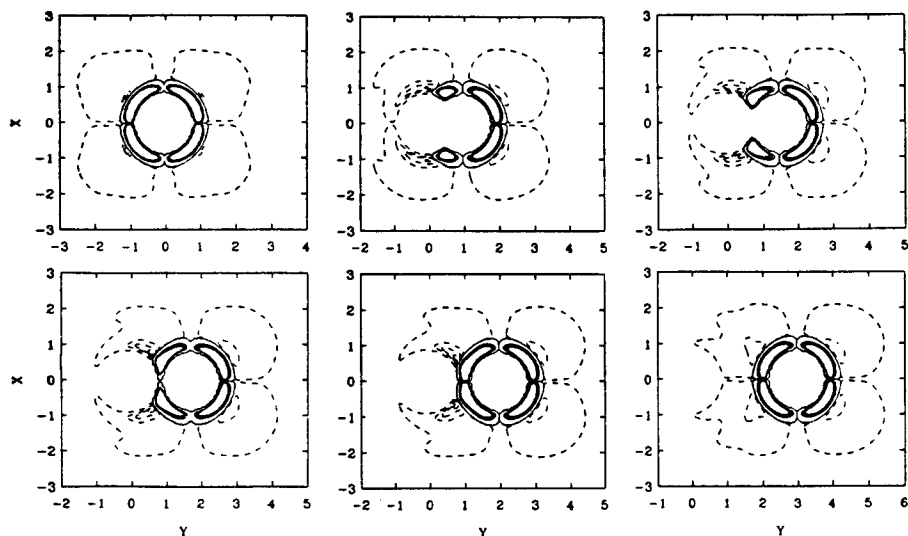


FIG. 11. Contour plot of the two-dimensional integrand of Eq. (A12) for six solute separations  $r = 0.0, 1.0, 1.25, 1.5, 1.75$  and  $2.0 \sigma$ ; i.e., from the first to the second solvation shell. Solid lines indicate positive levels and dashed lines negative levels. The integrand represents the force-force fluctuation acting on the particle at  $(X=0, Y=r)$  in the presence of the second particle located at the origin.

$$= 2\pi\rho \int_0^\pi d\theta \sin\theta \int_0^\infty dr r^2 g(r) g[r_0(r, \theta)] \sum(r, \theta), \quad (\text{A11})$$

where we have invoked the Kirkwood superposition approximation<sup>19</sup> for the triplet correlation function  $g^{(3)}(r) = g(r)g(r_0)$  where the distance  $r_0$ , shown in Fig. 10, is defined  $r_0 = \|\mathbf{r}\| \sqrt{r^2 + a^2 + 2ra \cos\theta}$ .

The zero-time value of the memory function  $K(t=0)$  is the mean-square force divided by the mean-square momentum. The memory function is related to the time-dependent friction  $\zeta(t) = \mu K(t)$ . It follows that the zero-time value for the time-dependent friction is

$$\zeta(0) = \beta \hat{z} \cdot \left[ \langle \mathbf{F}_{AB}(\mathbf{r}_{AB}) \mathbf{F}_{AB}(\mathbf{r}_{AB}) \rangle - \langle \mathbf{F}_{AB}(\mathbf{r}_{AB}) \rangle \langle \mathbf{F}_{AB}(\mathbf{r}_{AB}) \rangle \right] \cdot \hat{z}, \quad (\text{A12})$$

where  $\mu$  is the reduced mass of the pair of atoms A and B. The integrals were performed by quadrature. Results are plotted in Fig. 6 as a function of the interparticle separation ( $x$ ) and compared with the results of our simulation.

The qualitative agreement of the superposition approximation with the simulation values observed in Fig. 6 is indicative that Eq. (A12) may be used as a useful tool to analyze the distance dependence of the force-force fluctuation. The integrand of Eq. (A12), reduced to two dimensions from the cylindrical symmetry, is plotted in Fig. 11 at constant contour levels for different solute-solute separations. It is clear that the presence of a second solute introduces a shielding from the solvent particles as the solute separation increases from 1.0 to 2.0  $\sigma$ . The results are discussed further in Sec. IV.

<sup>1</sup> B. J. Berne and G. D. Harp, *Adv. Chem. Phys.* **17**, 63 (1970).

<sup>2</sup> P. Hanggi, P. Talkner, and M. Borkovec, *Rev. Mod. Phys.* **62**, 251 (1990).

<sup>3</sup> B. J. Berne, M. E. Tuckerman, J. E. Straub, and A. L. R. Bug, *J. Chem. Phys.* **93**, 5084 (1990).

<sup>4</sup> J. E. Straub, M. Borkovec, and B. J. Berne, *J. Phys. Chem.* **91**, 4995 (1987).

<sup>5</sup> J. E. Straub, M. Borkovec, and B. J. Berne, *J. Chem. Phys.* **89**, 4833 (1988).

<sup>6</sup> M. G. Sceats, *Chem. Phys. Lett.* **128**, 55 (1986).

<sup>7</sup> R. Zwanzig, *J. Stat. Phys.* **9**, 215 (1973).

<sup>8</sup> B. J. Berne and R. Pecora, *Dynamic Light Scattering* (Wiley-Interscience, New York, 1976).

<sup>9</sup> J. Metiu, D. W. Oxtoby, and K. F. Freed, *Phys. Rev. A* **15**, 361 (1977).

<sup>10</sup> In a study of vibrational relaxation of a diatomic in a liquid, Freed and coworkers (Ref. 9) assumed that the time-dependent friction acting on the stretching coordinate of the diatomic was approximately one-half the friction acting on a single atom. We have tested that approximation in a study of a simple reaction of a diatomic in a liquid (Ref. 5) and found it to be reasonable for separations  $r \approx \sigma$ .

<sup>11</sup> B. J. Berne, in *Multiple Time Scales*, edited by J. U. Brackbill and B. I. Cohen (Academic, New York, 1985).

<sup>12</sup> R. F. Grote and J. T. Hynes, *J. Chem. Phys.* **77**, 3736 (1982).

<sup>13</sup> B. Carmeli and A. Nitzan, *Phys. Rev. Lett.* **49**, 423 (1982).

<sup>14</sup> S. A. Adelman, *Adv. Chem. Phys.* **53**, 61 (1983).

<sup>15</sup> J. T. Hynes in *Theory of Chemical Reaction Dynamics*, edited by M. Baer (CRC Press, Boca Raton, FL, 1985), p. 171.

<sup>16</sup> D. E. Smith and C. B. Harris, *J. Chem. Phys.* **92**, 1312 (1990).

<sup>17</sup> R. F. Grote and J. T. Hynes, *J. Chem. Phys.* **73**, 2715 (1980).

<sup>18</sup> H. A. Kramers, *Physica* **7**, 284 (1940).

<sup>19</sup> D. A. McQuarrie, *Statistical Mechanics* (Harper and Row, New York, 1976).

<sup>20</sup> J. A. McCammon, S. H. Northrup, and S. A. Allison, *J. Phys. Chem.* **90**, 3901 (1986).

<sup>21</sup> G. D. Harp and B. J. Berne, *Phys. Rev. A* **2**, 975 (1970).

<sup>22</sup> C. L. Brooks and S. A. Adelman, *J. Chem. Phys.* **77**, 4845 (1982).

<sup>23</sup> S. W. Haan, *Phys. Rev. A* **20**, 2516 (1979).

<sup>24</sup> U. Balucani, R. Vallauri, and C. S. Murthy, *J. Chem. Phys.* **77**, 3233 (1982).

<sup>25</sup> C. Hoheisel and M. D. Zeidler, *Mol. Phys.* **54**, 1275 (1985).

<sup>26</sup> P. L. Fehder, C. A. Ermeis, and R. P. Futrelle, *J. Chem. Phys.* **54**, 4921 (1970).

<sup>27</sup> The second, based on modeling reactions, depends on a differential fractal dimension  $d$  and is written (Ref. 33)

$$D(r) = \frac{k_B T}{\zeta} \frac{1}{1 + d/r}. \quad (\text{A13})$$

The parameter  $d$  attempts to include contributions from dynamic correlations between the reactants and solvent. In the region of  $r \approx \sigma$ , Eq. (A13) is approximately the same as Eq. (5.2) where  $d = 0.1\sigma$ .

<sup>28</sup> S. H. Northrup and J. T. Hynes, *J. Chem. Phys.* **71**, 871 (1979).

<sup>29</sup> S. H. Northrup and J. T. Hynes, *J. Chem. Phys.* **71**, 884 (1979).

<sup>30</sup> R. I. Cukier, R. Kapral, and J. R. Mehafeey, *J. Chem. Phys.* **73**, 5254 (1980).

<sup>31</sup> M. Schell, R. Kapral, and R. I. Cukier, *J. Chem. Phys.* **75**, 5879 (1981).

<sup>32</sup> W. W. Wood, *Fundamental Problems in Statistical Mechanics, Vol. 3*, (North-Holland, Amsterdam 1975), p. 331.

<sup>33</sup> M. A. López-Quintela, M. C. Buján-Núñez, and J. C. Pérez-Moure, *J. Chem. Phys.* **88**, 7478 (1988).